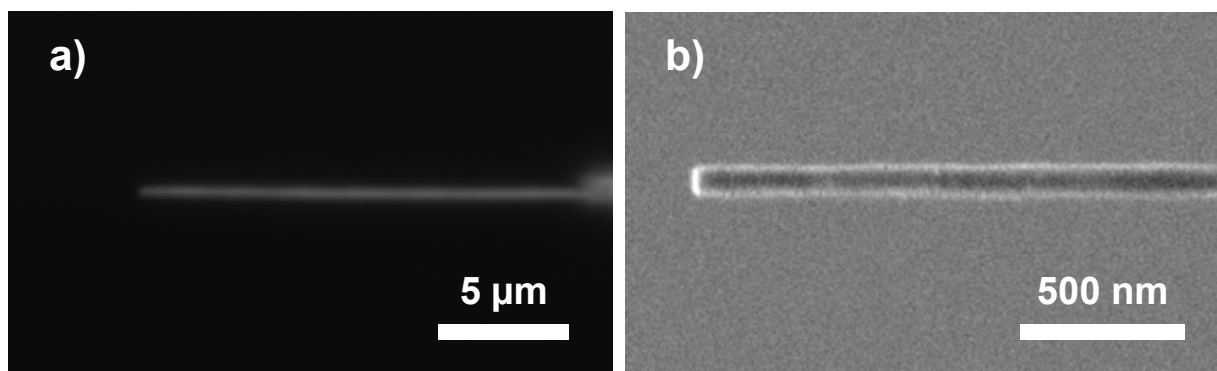


**Supporting Information for**  
**Electrochemically-Controlled Deconjugation and Delivery of Single Quantum**  
**Dots into the Nucleus of Living Cells**

Kyungsuk Yum, Ning Wang, Min-Feng Yu

Department of Mechanical Science and Engineering, University of Illinois at Urbana-Champaign,  
1206 West Green Street, Urbana, IL 61801 (USA)



**Figure S1.** a) Optical microscope image of a typical gold-coated nanoneedle. b) Scanning electron microscope image of a gold-coated nanoneedle.

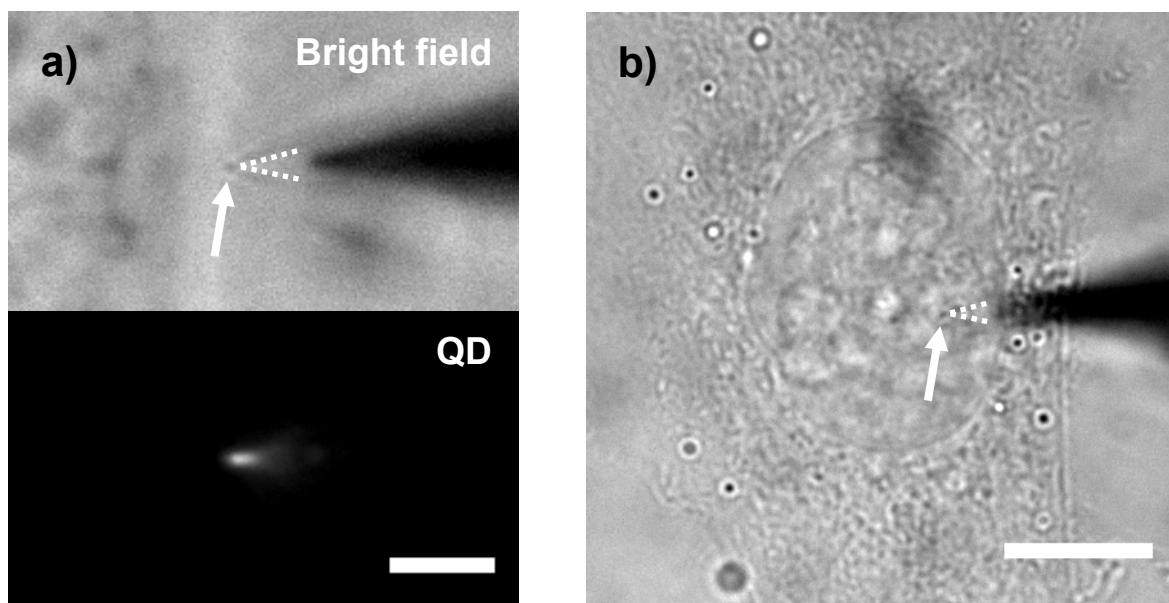


**Figure S2.** a) Bright-field (top) and fluorescence (bottom) images of a nanoneedle before penetrating into a cell for the delivery experiment. The target cell is shown on the left side of the nanoneedle; the cell is unfocused because it is below the nanoneedle. The QDs attached on the nanoneedle is shown in white. Scale bar, 5 μm. b) Image of the nanoneedle during the delivery experiment. The whole process is monitored under the direct visualization of the optical

microscope. The nanoneedle can be precisely located at the target release site in the three-dimensional cellular environment by focusing on the tip of the nanoneedle. The tip of the nanoneedle and the nuclear envelope is on the same focal plane. Scale bar, 10  $\mu\text{m}$ . The unfocused dark shade on the right side of the nanoneedle in (a) and (b) is the macroscopic needle on which the nanoneedle is attached. The arrow indicates the tip of the nanoneedle; the dotted line guides the nanoneedle, gradually unfocused from its tip.

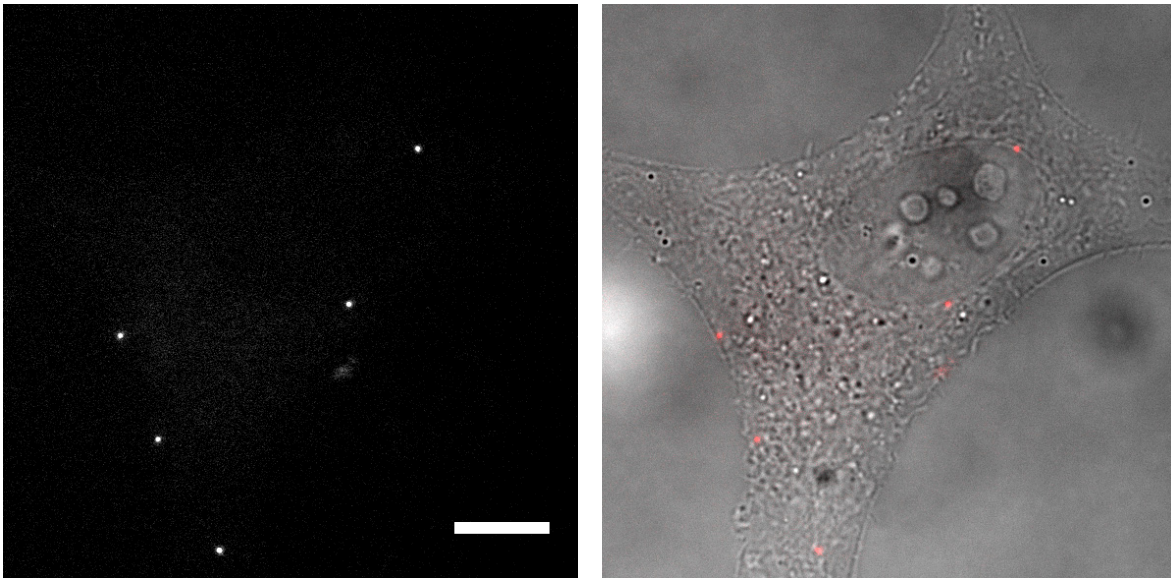


**Figure S3.** Delivery of QDs into the cytoplasm of a living HeLa cell: fluorescence image (left) and overlay of bright-field and fluorescence images (right) of the cell on a focal plane. Scale bar, 10  $\mu\text{m}$ .

### **Factors affecting the success rate of the delivery**

We detected QDs in about 60% of target cells after the delivery process (12 out of 21 cells). The failure in some cases is mostly due to the unreliable electric connection at the contact junction between the coated nanotube and the macroscopic metal wire (the electrochemically sharpened tungsten wire). As no electric potential can then be applied directly onto the nanoneedle, no electrochemical release of the quantum dots from such nanoneedles can be enabled. The fabrication process itself may introduce some unreliable electric connection, but mostly it is the mechanical bending or even buckling experienced by the nanoneedle during the immersion of the nanoneedle into the cell medium that degrades the electric connection at the contact junction [1-4]. The surface tension experienced by the nanoneedle during its entry to the cell medium is noticeable. Improving both the mechanical and electrical integrity of the contact junction between the nanoneedle and the macroscopic metal wire could potentially improve the success rate of the delivery. Another related cause affecting the success rate of the delivery is that not all QDs delivered into cells are fluorescent (the percentage can range from 30 to 70% according to literatures) [5, 6]. Considering also that only a small number of QDs are delivered in each delivery and tracking fast-moving single QDs in a three-dimensional cellular environment is generally difficult, we may not fully count all successful deliveries.

### **Charge Injection during the Delivery Process**

The number of charge injected into a cell by applying a potential ( $\sim 1.4$  V for 60 s) is estimated to be  $\sim 10^7$ , assuming a current density of  $\sim 10$   $\mu\text{A}/\text{cm}^2$  [7] and an effective electrode surface area of  $\sim 3 \times 10^{-9}$   $\text{cm}^2$  (for a nanoneedle end segment of  $\sim 50$  nm in diameter and  $\sim 2$   $\mu\text{m}$  in length that is functionalized with SAM and QDs). The number of thiols on the nanoneedle segment is  $\sim 10^6$ ,

assuming the surface density of thiols of  $7.7 \times 10^{-10}$  mol/cm<sup>2</sup> [8]. These numbers are only ~0.01–0.001% of the typical number of ions in a cell ( $\sim 10^{11}$ ); thus, their effect on the cellular environment is not substantial. Alternatively, to maintain the electrical neutrality of the intracellular environment, alternative pulses of positive and negative potentials can be applied during the release process. The strength of the electric field is  $\sim 1$  V/cm, much smaller than that used in electroporation ( $\sim 250$ – $750$  V/cm) [9].

### Supporting Movies

**Movie S1.** Movement of QDs delivered into the nucleus of a living HeLa cell. The speed of the movie is 2 $\times$ . The original acquisition time is 100 ms per image. The view size is  $15 \times 10$   $\mu$ m.

**Movie S2.** Fluorescence imaging of a single less-mobile QD in the nucleus of a living HeLa cell, indicated by the arrow in Figure 3a. The blinking of the QD suggests that it is mostly single. The time trace of the fluorescence intensity is shown in Figure 3b. The speed of the movie is 2 $\times$ . The original acquisition time is 100 ms per image. The view size is  $3 \times 3$   $\mu$ m.

### References

1. I. U. Vakarelski, S. C. Brown, K. Higashitani and B. M. Moudgil, *Langmuir*, 2007, **23**, 10893.
2. J. E. D. de Asis, Y. Li, R. Ohta, A. Austin, J. Leung and C. V. Nguyen, *Appl. Phys. Lett.*, 2008, **93**, 023129.
3. M. J. Esplandiu, V. G. Bittner, K. P. Giapis and C. P. Collier, *Nano Lett.*, 2004, **4**, 1873.
4. Y. Narui, D. M. Ceres, J. Chen, K. P. Giapis and C. P. Collier, *J. Phys. Chem. C*, 2009, **113**, 6815.

5. Y. Ebenstein, T. Mokari and U. Banina, *Appl. Phys. Lett.*, 2002, **80**, 4033.
6. J. Yao, D. R. Larson, H. D. Vishwasrao, W. R. Zipfel and W. W. Webb, *Proc. Natl. Acad. Sci. U. S. A.*, **102**, 14284.
7. F. Loglio, M. Schweizer, D. M. Kolb, *Langmuir* **2003**, *19*, 830.
8. P. Mali, N. Bhattacharjee, P. C. Searson, *Nano Lett.* **2006**, *6*, 1250.
9. J. Sambrook, D. W. Russell, *Molecular Cloning: A Laboratory Manual*, 3 ed., Cold Spring Harbor Laboratory Press, Cold Spring Harbor, New York, **2001**.